Chapter 4

Thermodynamic and Kinetic Study of Lignocellulosic Waste Gasification

Rosa Ana Rodriguez, Germán Mazza,

Marcelo Echegaray, Anabel Fernandez and

Daniela Zalazar García

Additional information is available at the end of the chapter

http://dx.doi.org/10.5772/intechopen.73288

Abstract

In this chapter, the kinetic behavior during the steam gasification of sawdust, plum, and olive pits was investigated by thermogravimetric analysis where the weight loss is measured with the temperature variation at different heating rates (5, 10, and 15 K/min). The weight loss and their derivative curves show that the gasification takes place in three visible stages. The kinetic study was carried out using Coats-Redfern methods. The Ginstling-Brounstein model showed better fit. The obtained activation energy values vary between 70 and 100 kJ/mol for the pyrolysis stage for all studied agro-industrial wastes. On the other hand, a thermodynamic model was proposed to predict the five waste gasification processes, considering the char and tar production. The proposed model allows it to perform a parametric study, analyzing the process variables' effect on the exergetic efficiency. The higher temperatures favor the endothermic reactions as the H_2 and CO formation reactions. Therefore, in the product, moles of H_2 and CO increase and consequently the exergy efficiency of the process. Increasing the equivalence ratio value, H_2, CO, and CH_4 contents decrease; thus the calorific value of the produced gas and the exergetic efficiency decrease. In addition, the CO_2 and H_2O presences in the syngas composition diminish its calorific value and the exergetic efficiency. Considering the influence of supply steam/biomass ratio, the exergetic efficiency decreases with the growth of this parameter.

Keywords: gasification, lignocellulosic wastes, kinetic analysis, thermodynamic analysis

1. Introduction

Energy demand has gradually become a critical factor for the international industrial sector. For this reason, technologies based on renewable-energy sources, such as biomass residues, have been developed and promoted. Biomass has the potential to become one of the main sources of energy worldwide; it is estimated that by 2050, its contribution to the global energy model could be between 100 and 400 EJ/year [1].

The biomass waste utilization, as a substitute for fossil biofuels, has the advantage to produce environmentally beneficial fuel, due to the energy production, and its sustainable use allows the emitted CO_2 to be absorbed during the biomass growth. In short time periods, this cycle was fulfilled, which allows confirming that the energetic biomass uses under these conditions in neutral with respect to the CO_2 emissions [2]. One of the main disadvantages for the biomass waste utilization is its low production per unit area, causing high costs related with the collection and the transport from the origin to the consumption place [3]. Due to this reason, the systems using biomass must have a high efficiency.

Recently, to develop the energy obtaining from waste biomass, several works have been carried out; particularly about pyrolysis and gasification because these thermal processes are effective and attractive methods [4, 5]. Considering the gasification, it converts biomass wastes into low heating value gas generally called syngas. This product is more suitably used to produce electricity through internal combustion engines or gas turbines [6].

Different operating variables have a high influence on the gasification behavior: biomass feedstocks, temperature (T), equivalence ratio (ER, supply air/stoichiometric air), and supply steam/biomass ratio (SBR) [7]. In order to evaluate the gasification performance, the exergy analysis can be employed (based on the second law of thermodynamic).

On the other hand, considering the kinetic behavior, the biomass waste gasification occurs in three stages: drying (evaporation of moisture contained in the solid), pyrolysis (thermal decomposition in the oxygen absence), and the last step associated with the reaction of the char by CO_2 to produce CO. When the solid fuel is heated to temperatures between 473 and 648 K in the absence of an oxidant agent, it is pyrolyzed. The process products are a solid (char), condensable hydrocarbons (tar), and gases. Then, at higher temperatures, the condensable fraction and the gases form part of the volatile phase of the pyrolysis. The additional permanence of the solid and volatile phases in the reaction zone allows their conversion to a fraction of gases (gasification) [8].

The tar presence in the gas mixture is the main problem in the technological development of the gasification systems of biomass. The generated char during the pyrolysis stage can react with water vapor, CO_2, and oxygen. These reactions occur slower than that corresponding to the volatile phase; however, these contribute significantly to increase the amount and calorific value of the syngas.

Considering the gasification process description above, the involved reaction number, and their unknown mechanisms, simple kinetic models cannot describe the global reactions.

In this chapter, the kinetic characterization of different lignocellulosic waste gasification processes by thermogravimetric techniques using the Coats-Redfern method is presented [8]. The experimental data were fitted with several models, and each one was evaluated with different statistical parameters. Using the model with the best fit, the activation energy and pre-exponential factor were calculated, and their variation with the heating rate was evaluated [9]. On the other hand and in order to extend and improve the basic knowledge on composition and properties and to apply this knowledge for the most advanced and environmentally safe utilization, an exergy analysis of a gasification process is presented, taking into account different byproducts' production.

2. Kinetic analysis

Coats and Redfern [8] method has been widely applied to study the thermal decomposition kinetics of biomass. The reaction kinetic equation is

$$d\alpha/dt = k(T)\, f(\alpha) \tag{1}$$

where k(T) is the rate constant, $d\alpha/dt$ is the process rate, T is the absolute temperature, t is the time, $f(\alpha)$ represents function commonly used for description of biomass thermal decomposition, and α is the degree of transformation; α can be calculated from the corresponding TG curve by the following equation:

$$\alpha = (m_0 - m)/(m_0 - m_f) \tag{2}$$

$$\beta = dT/dt \tag{3}$$

where m is the mass of the sample at a given time t and m_0 and m_f refer to values at the initial and final mass of samples. For non-isothermal conditions, when the temperature varies with time with a constant heating rate defined by

$$k = A \exp(-E/RT) \tag{4}$$

According to Arrhenius expression:

where A is the pre-exponential factor, E is the activation energy, and R is the universal gas constant.

After a combination of Eqs. (1) and (4) and integrating, the following expression is obtained:

$$g(\alpha) = \int_0^{\alpha} d\alpha/f(\alpha) = (A/\beta) \int_0^{T} e^{(-E/RT)}\, dT \tag{5}$$

Eq. (5) can be integrated when the right hand side is expanded into an asymptotic series and higher order terms are ignored:

$$g(\alpha)/T^2 = \left(AR/E\beta\right)\left[\left(AE/E\beta\right) - (1 - 2RT/E)\right] - (E/RT) \quad (6)$$

The term 2RT/E can be neglected since it is much less than unity for the thermal decomposition of lignocellulosic materials. Plotting the left hand side of Eq. (6), which includes $g(\alpha)/T^2$ versus T, for the proposed models (**Table 1**), gives the E and A parameters. The least squares nonlinear regression was used by means of the Marquardt [10] and Levenvrg [11] algorithm using MATLAB software.

Table 1 lists several reaction models ($g(\alpha)$) used in this work to describe biomass thermal decomposition.

Reaction model	**g(α)**
Reaction order	
Zero order	α
First order	$-\ln(1-\alpha)$
Nth order	$(n-1)-1\ (1-\alpha)1-n$
Diffusional	
One-dimensional diffusion	$\alpha 2$
Two-dimensional diffusion	$(1-\alpha)\ln(1-\alpha)+\alpha$
Three-dimensional diffusion (Jander)	$[1-(1-\alpha)1/3]2$
Three-dimensional diffusion (Ginstling-Brounstein)	$(1-2\alpha/3)-(1-\alpha)2/3$
Nucleation	
Power law	αn n = 3/2, 1, ½, 1/3, 1/4
Exponential law	α
Avrami-Erofeev	$[-\ln(1-\alpha)](1/n)$, n = 1, 2, 3, 4
Contracting geometry	
Contracting area	$(1-\alpha)(1/n)$, n = 2
Contracting volume	$(1-\alpha)(1/n)$, n = 3

Table 1. Expressions for the most common reaction mechanisms in solid-state reactions.

3. Thermodynamic model

The proposed model in this work is derived from the thermodynamic equilibrium applying the following assumptions:

- The gasifier is considered as a system in stationary state, with homogeneous temperature and pressure.
- The C content in the biomass is converted in gases due to the gasification and combustion processes, and it can remain in the fly and bottom ash like char. The considered gaseous

products are CO, H_2, CO_2, CH_4, H_2O, and N_2. The quantities of other produced hydrocarbons are considered negligible. The tar production is considered in this model.

- The ash contents in the studied biomass are considered inert during all the process reactions.
- All gaseous products behave as ideal gases. This assumption error is not significant for the gasifiers operating at low pressure and high temperature.
- The S, Cl, and N contents in the biomass are negligible because they are very low compared with the C, H, and O contents.

The biomass is represented by the general formula CH_aO_b obtained from elemental analysis. The gasification process of the regional wastes can be characterized by the following global reaction:

$$\begin{aligned} CH_aO_b + wH_2O + m(O_2 + 3.76N_2) \rightarrow x_1CO + x_2H_2 + x_3CO_2 \\ + x_4H_2O + x_5CH_4 + x_6C + m3.76N_2 + x_{tar}CH_{1.003}O_{0.33} \end{aligned} \quad (a)$$

where w is the water mol/biomass mol; m is the air mol/biomass mol; x_1, x_2, x_3, x_4, and x_5 are unknown moles of exit gas composition; and x_6 and x_{tar} are char and tar exit moles, respectively.

Zainal et al. [12] presented a representative tar composition; this composition was used in this work. w and m are determined as function of the steam/biomass ratio (SBR, kg/kg) and ER (oxygen/biomass ratio, kmol/kmol). So, w and m expressions are

$$w = (SBR + w_w) \cdot \frac{M_{bm}}{18} \quad (7)$$

$$m = ER \cdot \left(1 + \frac{a}{4} - \frac{b}{2}\right) \quad (8)$$

where w_w is the mass faction of moisture content in the biomass and M_{bm} is reactant biomass quantity expressed as kmol of dry biomass/h:

$$M_{bm} = \frac{12 + a + 16b}{1 - w_w} \quad (9)$$

Taking into account global reaction (a), the balances for C, H, and O are

$$x_1 + x_3 + x_5 + x_6 + x_{tar} = 1 \quad (10)$$

$$a + 2w = 2x_2 + 2x_4 + 4x_5 + 1.003x_{tar} \quad (11)$$

$$b + w + 2m = x_1 + 2x_3 + x_4 + 0.33x_{tar} \quad (12)$$

Zainal et al. [12] considered the following reactions:

Water-gas-shift reaction:

$$CO + H_2O \overset{K_{wgs}}{\longleftrightarrow} CO_2 + H_2 \quad (b)$$

Methane reaction:

$$C + 2H_2 \overset{K_{methan}}{\longleftrightarrow} CH_4 \tag{c}$$

In these reactions, the oxygen is not involved directly, and the steam is implicated in a limited form (water-gas-shift reaction). So, the gasifying agent's effect on the equilibrium reactions is not important. The equilibrium constants as partial pressure function are

$$K_{wgs} = \frac{p_{CO_2} \cdot p_{H_2}}{p_{CO} \cdot p_{H_2O}} = \frac{x_2 \cdot x_3}{x_1 \cdot x_4} \tag{13}$$

$$K_{methan} = \frac{p_{CH_4}}{p_{H_2}^2} p_0 = \frac{x_5}{x_2^2} \frac{p_0}{p} x_{total} \tag{14}$$

where p and p_0 are the total and reference pressures, respectively. They are equal to 101.3 kPa. x_{total} is the mol quantity of produced gas, excluding the inert gas.

The variation of Gibbs free energy at a determined temperature was used in order to know the K_{wgs} and K_{methan} values, according to the following equations:

$$\ln K(T) = \frac{-\Delta G_T^0}{RT} \tag{15}$$

$$\Delta G_T^0 = \sum_i \nu_i \cdot \Delta G_{f,i,T}^0 \tag{16}$$

where $\Delta G_{f,i,T}^0$ is the free energy of each constituent formation at a temperature equal T, ΔG_T^0 is the standard free energy at a temperature equal T, and ν_i is the stoichiometric number of the reaction products.

The necessary thermodynamic data were obtained of Reid, Prausnitz, and Polling [13]. The equilibrium constants as temperature function can be expressed by

$$K_{wgs} = EXP\left(\frac{5872.45}{T} + 1.86 \ln T - 2.69 \cdot 10^{-4} T - \frac{58200}{T^2} - 18\right) \tag{17}$$

$$K_{methan} = EXP\left(\frac{7082.842}{T} - 6.567 \ln T + \frac{7.467 \cdot 10^{-3}}{2} T - \frac{2.167 \cdot 10^{-6}}{6} T^2 + \frac{0.701 \cdot 10^{-5}}{2T^2} + 32.541\right) \tag{18}$$

3.1. Nonequilibrium factors

The assumed thermodynamic equilibrium for these reactions is not valid for real process due to the reactions that are not complete and the mass transfer resistance, too [14]. The equilibrium constant is modified to consider the nonequilibrium behavior:

$$K_{wgs}^* = K_{wgs} \cdot f_{wgs} \tag{19}$$

$$K_{methan}^* = K_{methan} \cdot f_{methan} \tag{20}$$

where f_{wgs} and f_{methan} are the nonequilibrium factors of the water-gas displacement and methanation reactions, respectively. Lim and Lee [14] obtained the values of these factors analyzing the T, ER, and SBR influences on them, considering several biomasses. Thereby, two empirical equations of f_{wgs} and f_{methan} are obtained:

$$f_{wgs} = 0.0836 \cdot e^{2.882 \cdot ER} \tag{21}$$

$$f_{methan} = 38.75 - 30.70 \cdot ER \tag{22}$$

f_{wgs} is smaller than 0.5, and this reaction is close by to equilibrium. Since the CO production during the gasification decreases when ER increases, f_{wgs} augments with this parameter in order to promote the water-gas displacement reaction. However, ER significantly affects f_{methan} varying between 20 and 33 approximately [14].

3.2. C conversion fraction

C is partially converted into gas under substoichiometric conditions, and it is related with O concentration in the atmosphere and the gasification temperature. C conversion fraction (f_c) is defined as the ratio between the mol total number in the gas composition and the C concentration present in the biomass. The non-converted C will be [14]

$$x_6 = 1 - f_c \tag{23}$$

$$f_c = 0.901 + 0.439 \cdot \left(1 - e^{(-ER + 0.0003 \cdot T)}\right) \tag{24}$$

The empirical parameters of these correlations were determined considering the experimental results obtained during the biomass gasification using air/steam mixture as gasifier agent [14].

3.3. Tar formation

Abuadala [15] defined the tar yield as a percentage by weight of the total gasification products:

$$Tar_{wt,\%} = 35.98e^{(-0.00298 \cdot T)} \tag{25}$$

The total weight of gasification products is obtained applying a global mass balance. The tar mass is obtained by

$$m_{tar} = \frac{Tar_{wt,\%}}{100}(M_{bm} + SBR \cdot M_{bm} + w_w \cdot M_{bm} + 29(m + 3.76m)) \tag{26}$$

where M_{bm} and w_w are the fed biomass mass flow and moisture fraction of fed biomass (dry basis), respectively. The tar moles can be calculated by

$$x_{tar} = \frac{m_{tar}}{PM_{tar}} \tag{27}$$

where PM_{tar} is the tar molecular weight. In this case, the considered tar chemical formula is

$CH_{1.003}O_{0.33}$ proposed by Allesina et al. [16]. Considering Eqs. (5)–(7), (13)–(15), (17), and (21), the syngas composition can be obtained as operative variable function, T, ER, and SBR.

3.4. Process performance condition

The performance condition used in this work is the exergetic efficiency (η_{ex}). It is defined as the ratio between the profitable exergy outputs flow from the gasifier and the necessary exergy input flow to the gasifier [18]:

$$\eta_{ex} = \frac{\varepsilon x_{gas} + \varepsilon x_{loss} + \varepsilon x_{tar} + \varepsilon x_{char}}{\varepsilon x_{biomass} + \varepsilon x_{steam}} \tag{28}$$

where εx_{loss}, is the loss exergy flow and, εx_{gas}, εx_{tar}, εx_{char}, $\varepsilon x_{biomass}$, and εx_{steam} are the loss exergy flow and exergy flows of gas, tar, char, biomass, and steam, respectively. There is a loss due to the entropy production, heat and mass transfers, and chemical reaction irreversibility [18]. Considering the gasification process, it must satisfy the first and second thermodynamic laws. The second law leads to the following expression:

$$\sum_{R} \varepsilon x - \sum_{P} \varepsilon x = I \tag{29}$$

where εx is the exergy and I is the irreversibility, and it represents the lost internal exergy as the material quality loss and energy due to dissipation. It is calculated basing to the generated entropy during the gasification process:

$$I = T^{\circ} \cdot Sgen \tag{30}$$

The exergy depends on the biomass composition (chemical exergy), temperature, and pression (physical exergy). The chemical exergy (εx_{ch}) can be calculated by

$$\varepsilon x_{ch} = \sum_{i} x_i \cdot \varepsilon x^{\circ}_{ch,i} + RT^{\circ} \sum_{i} x_i \cdot \ln x_i \tag{31}$$

where xi and $\varepsilon x^{\circ}_{ch,i}$ are the molar fraction and standard exergy of i species [19]. The produced gaseous and tar physical exergies (εx_{ph}) can be calculated by

$$\varepsilon x_{ph} = \left(H - H^{\circ}\right) - T^{\circ}\left(S - S^{\circ}\right) \tag{32}$$

where H and S are the enthalpy and entropy of a species when the gasifier operates at determined T and pression and H° and S° are the enthalpy and entropy when the reactor works under standard conditions (T° = 298 K and p° = 1 atm). The total exergy is

$$\varepsilon x = \varepsilon x_{ch} + \varepsilon x_{ph} \tag{33}$$

In order to carry out the analysis of the first and second thermodynamic laws, the entropy and

enthalpy values are necessary. The specific heat capacity of tar (kJ/kgtar·K) from biomass gasification process is [20]

$$Cp = 0.00422 \cdot T \tag{34}$$

The tar enthalpy and the entropy are calculated with the following expression [21]:

$$H_{tar} = H^{\circ}_{tar} + \int_{T^{\circ}}^{T} Cp \cdot dT \tag{35}$$

$$H^{\circ}_{tar} = -30.980 + x_{CO_2} \cdot H^{\circ}_{CO_2} + x_{H_2O} \cdot H^{\circ}_{H_2O} \tag{36}$$

where x_i and $H^{\circ}{}_i$ are the molar fraction and the standard formation enthalpy of i species, respectively. The tar entropy is

$$S_{tar} = S^{\circ}_{tar} + \int_{T^{\circ}}^{T} \frac{Cp}{T} \cdot dT \tag{37}$$

where S°_{tar} is the tar standard entropy (kJ/kmol·K), and it is calculated using the following expression:

$$\begin{aligned} S^{\circ}_{tar} = \; & 37.1636 + (-31.4767)\exp\left[-0.564682\left(\frac{H}{C} + N\right)\right] \\ & +20.1145\left(\frac{O}{C+N}\right) + 54.3111\left(\frac{N}{C+N}\right) + 44.6712\left(\frac{S}{C+N}\right) \end{aligned} \tag{38}$$

where C, H, N, O, and S are the weight fraction of carbon, hydrogen, nitrogen, oxygen, and sulfur present in the biomass, respectively. Usually, the gasifier losses at the environment are negligible comparing with the incoming and leaving energy of the gasifier. Several researchers consider that these losses are between 1 and 2% [22]. On the other hand, it is assumed that the char is pure carbon. Its specific heat capacity (kJ/kmol·K) is

$$Cp = 17.166 + 4.271\frac{T}{1000} - \frac{8.79 \cdot 10^5}{T^2} \tag{39}$$

The char chemical exergy is equal to 410 kJ/kmol, according to Moran and Shapiro [19]. Cengel [23] listed the values of standard enthalpy, entropy, and chemical exergy for the gaseous components. The biomass wastes are fed at environment temperature; its physical exergy is negligible. Ptasinski [24] calculated the biomass chemical exergy according to the expression present:

$$\varepsilon_{ch,\,biomass} = m_{biomass} \cdot \beta \cdot LHV_{biomass} \tag{40}$$

β factor is calculated by the following Eq. (24):

$$\beta = \frac{1.0414 + 0.0177\left(\frac{H}{C}\right) - 0.3328\left(\frac{O}{C}\right)\left(1 + 0.0537\left(\frac{H}{C}\right)\right)}{1 - 0.4021\left(\frac{O}{C}\right)} \tag{41}$$

Similarly, the tar chemical exergy is calculated using the liquid combustible correlation [25]:

$$\varepsilon_{ch,\,tar} = LHV_{tar}\left[1.0401 + 0.1728\left(\frac{H}{C}\right) + 0.0432\left(\frac{O}{C}\right)\right] \tag{42}$$

To evaluate the biomass high heating value (HHV,MJ/kg), the correlations presented by Sheng and Azevedo [26] were used, Eq. (1). The biomass low heating value (MJ/kg) is calculated with the following expression:

$$LHV_{biomass} = HHV_{biomass}(1 - w_w) - 2.447 \cdot w_w \tag{43}$$

2 MJ/kg is the latent heat of water vaporization at 298 K. In order to calculate the tar HHV, the following correlation is applied [27]

$$HHV_{tar} = 340.95\ C + 1322.98\ H - 119.86\ O \tag{44}$$

According to Richard and Thunman [28], the tar mass fraction of C, H, and O fractions of the tar are 0.545, 0.065, and 0.39, respectively.

4. Kinetic model application to biomass gasification

4.1. Experimental weight loss

The experiments were carried out in a tubular reactor of 5 cm of internal diameter and 100 cm of height. It is heated by electrical resistance and is coupled to an analytical balance. This equipment is connected to a control system, through which it is possible to vary the heating rate and to register time, mass data, and temperature in a computer.

Experiments were carried out under air/steam atmosphere; the steam flow rate was 0.17 ml/min, guarantying the steam/biomass ratio equal to 2.5 [7, 17]. The temperature increased from ambient temperature (approximately 300 K) to 1173 K. This final temperature ensures the highest decomposition. Three heating rates, 5, 10, and 15 K/min, were used. In order to minimize heat transfer and mass phenomena, 5 g of sample with size between 0.212 and 0.250 mm was used. **Figures 1–3** show these experiments.

4.2. Kinetic parameter determination

To determinate of kinetic parameters for the two stages, such as E and A, the weight loss curves have been used. Eq. (6) was applied to the experimental data, and a plot of $g(\alpha)/T^2$ versus T for

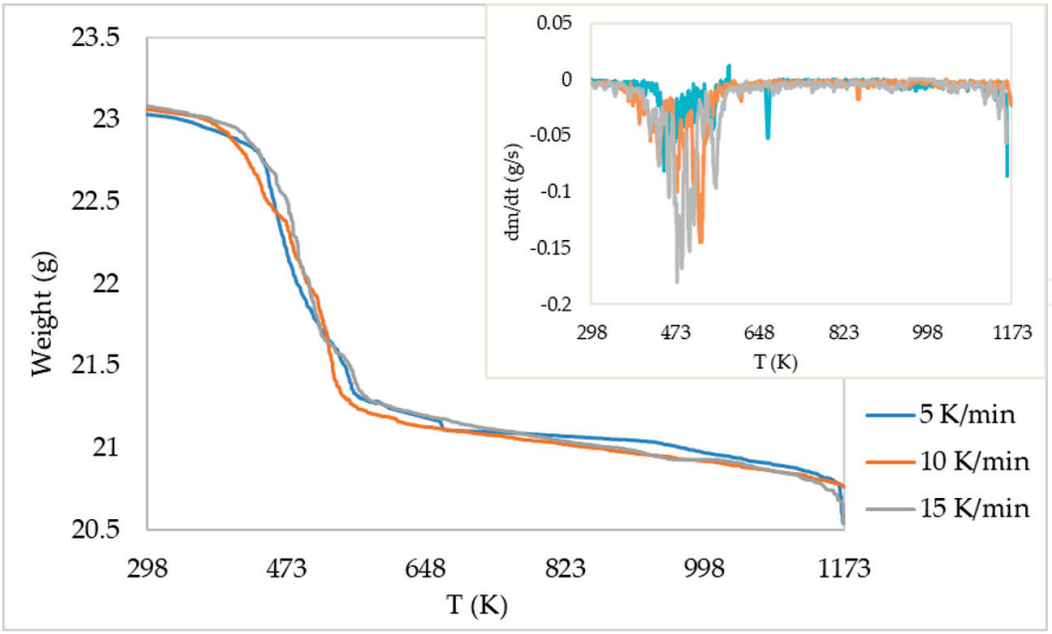

Figure 1. Weight loss and derivative curves for sawdust at different heating rates.

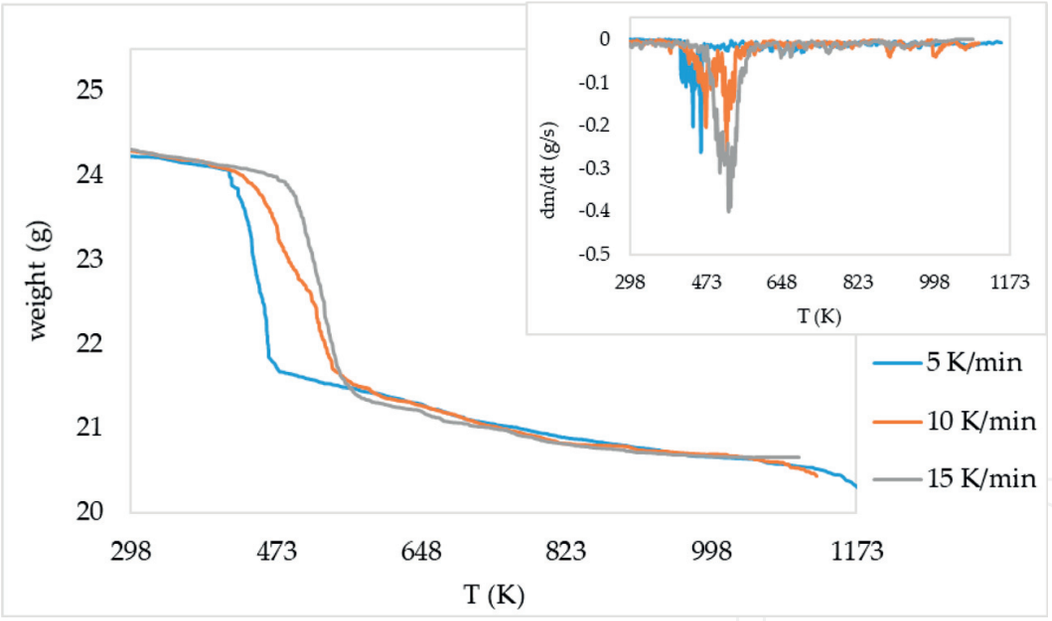

Figure 2. Weight loss and derivative curves for plum pits at different heating rates.

each biomass was obtained. **Figures 4–6** show the comparison of experimental data and the predicted values at different heating rates for the pyrolysis stage. The coefficient of correlation (R^2) for all cases is higher than 0.90, indicating a good fit.

The Ginstling-Brounstein model showed the better fit, and the obtained results are shown in **Table 2**.

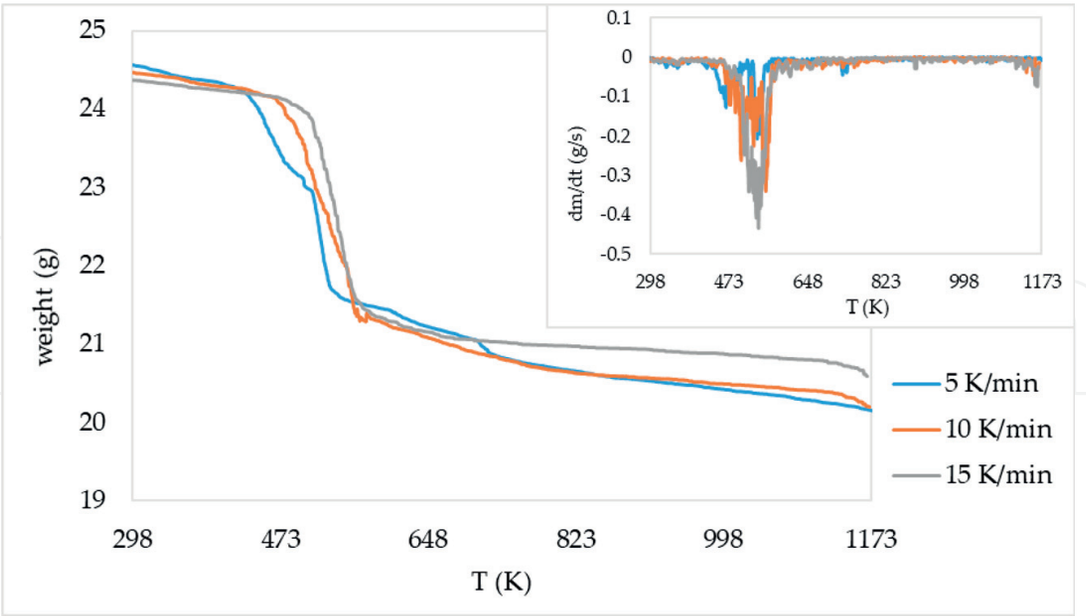

Figure 3. Weight loss and derivative curves for olive pits at different heating rates.

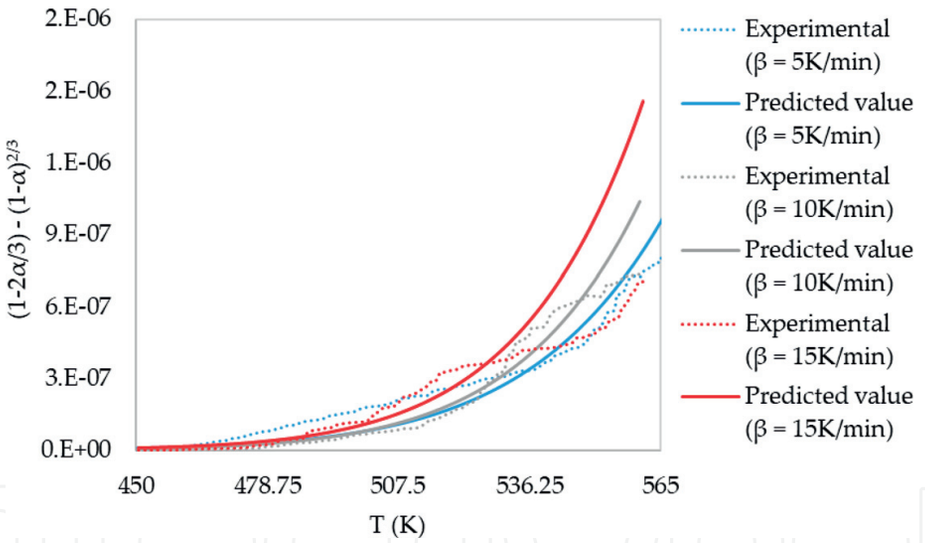

Figure 4. Comparison of experimental and predicted values of g(a) for sawdust at different heating rates for pyrolysis stage.

Figures 7–9 show the comparison of experimental data and the predicted values at different heating rates for the char combustion stage. The Ginstling-Brounstein model showed the better fit too, and the obtained results are shown in **Table 3**.

This model describes the biomass waste gasification characteristics, and it assumes that the process rate is limited by the diffusion of the reaction products from the surface, the reaction surface decreases during the process, and it can be assumed that the solid phase has the form of ball-shaped grains [29].

http://dx.doi.org/10.5772/intechopen.73288

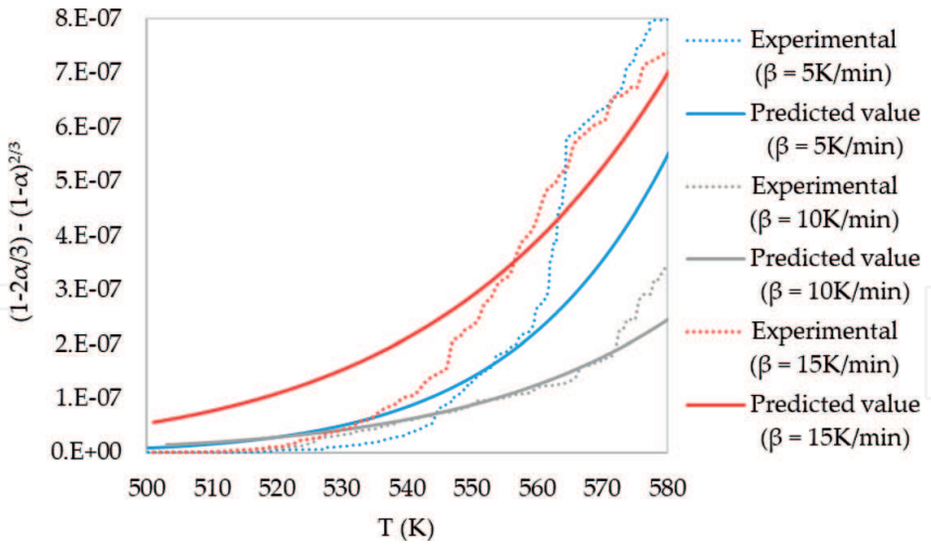

Figure 5. Comparison of experimental and predicted values of g(a) for plum pits at different heating rates for pyrolysis stage.

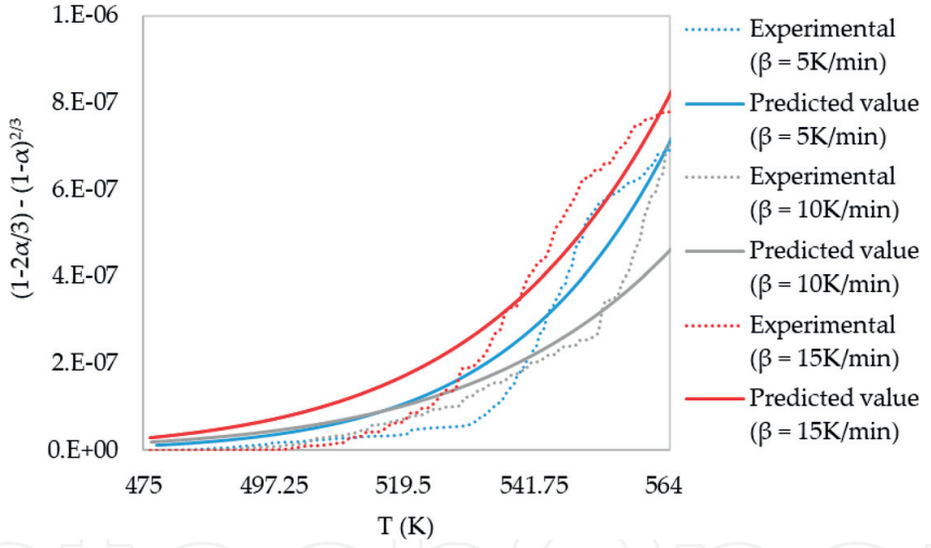

Figure 6. Comparison of experimental and predicted values of g(a) for olive pits at different heating rates for pyrolysis stage.

The obtained activation energy values vary between 70 and 100 kJ/mol and 24–98 kJ/mol for the pyrolysis and char gasification stages, respectively, for all studied agro-industrial wastes. The highest value of the energy activation was predicted for plum pits at heating rate of 15 K/min for pyrolysis stage. Also, the highest value for the same parameter was predicted for sawdust at 5 K/min for char combustion stage. The calculated values of E vary slightly with the heating rate for each biomass and indicate the existence of a complex multistep mechanism that occurs in the solid state. The increasing of heating rate leads to a simultaneous increase of the heat effect. So, the maximum decomposition rate tends to increase at higher heating rates because it provides a greater thermal energy facilitating the heat transfer around and

Agro-industrial wastes	Heating rate	Temp range	Kinetics parameters		Statistical parameters	
	β (K/min)	(K)	E (KJ/mol)	A (s−1)	R2	σ
Sawdust	5	450 565	90.96	1.34×10^{7}	0.90	7.31×10^{-8}
	10	450 560	98.62	1.91×10^{8}	0.98	3.44×10^{-8}
	15	442 561	99.80	5.10×10^{8}	0.91	6.13×10^{-8}
Plum pits	5	400 480	81.42	1.94×10^{7}	0.97	4.27×10^{-8}
	10	503 620	90.66	3.92×10^{6}	0.99	1.96×10^{-8}
	15	555 644	99.88	6.26×10^{6}	0.91	8.91×10^{-8}
Olive pits	5	387 477	70.23	1.59×10^{6}	0.91	7.09×10^{-8}
	10	476 679	80.45	1.22×10^{6}	0.98	3.21×10^{-8}
	15	488 578	87.46	1.07×10^{7}	0.92	8.91×10^{-8}

Table 2. Pre-exponential factor and activation energy obtained and the statistical parameter values for pyrolysis stage.

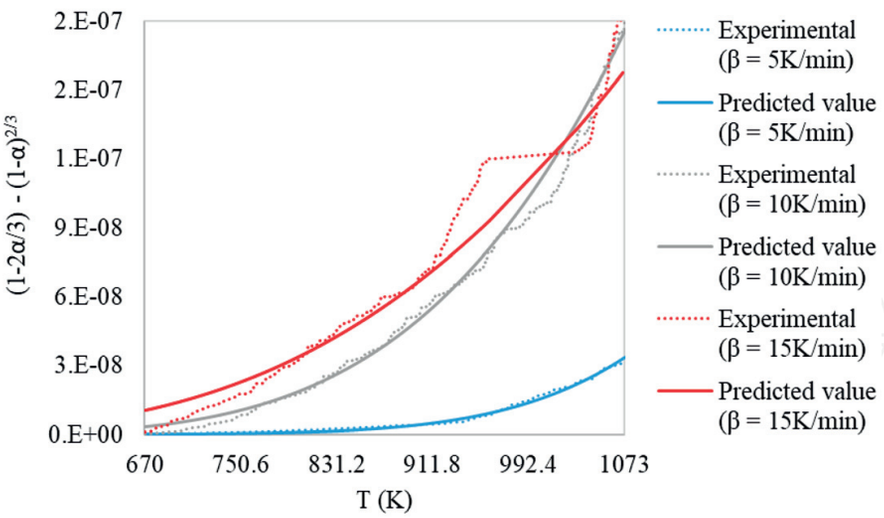

Figure 7. Comparison of experimental and predicted values of g(a) for sawdust at different heating rates for char gasification stage.

within the samples [30, 31]. The smallest value of this parameter was calculated for olive pit at 5 K/min. The found activation energy values are similar to obtained values by other authors [30, 32].

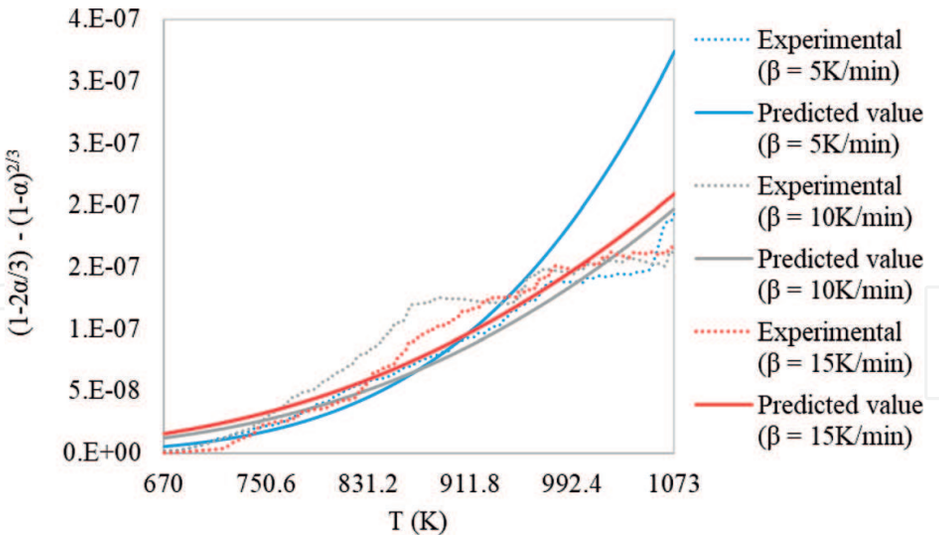

Figure 8. Comparison of experimental and predicted values of g(a) for plum pits at different heating rates for char gasification stage.

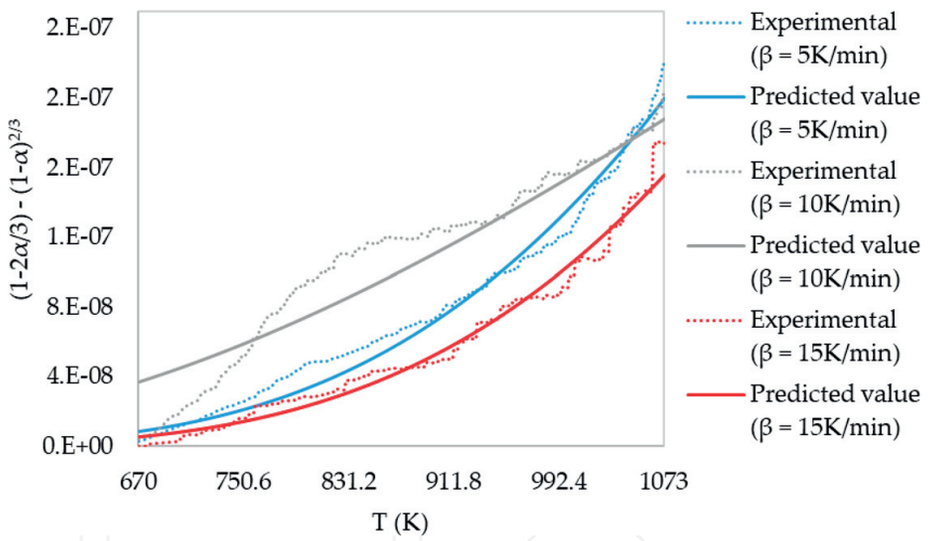

Figure 9. Comparison of experimental and predicted values of g(a) for olive pits at different heating rates for char gasification stage.

On the other hand, the pre-exponential factor value was obtained for each agro-industrial waste at the different heating rates. This parameter varies too with the heating rate; however, it is important to consider that it was obtained from a model-based method and it is tainted by association with the reaction model that must be assumed to permit its calculation.

5. Exergetic analysis to biomass gasification

The syngas composition and exergetic efficiency of the gasification process were studied with the lignocellulosic waste composition, gasifier temperature, and *ER* and *SBR* variation. *ER* was

Agro-industrial wastes	Heating rate	Temp range	Kinetics parameters		Statistical parameters	
	β (K/min)	(K)	E (KJ/mol)	A (s−1)	R2	σ
Sawdust	5	670 1073	98.19	1.20×10^{2}	0.97	2.85×10^{-9}
	10	670 1073	58.17	8.33×10^{0}	0.99	4.32×10^{-9}
	15	670 1073	40.11	1.03×10^{0}	0.95	6.67×10^{-9}
Plum pits	5	670 1073	60.25	1.00×10^{1}	0.90	8.15×10^{-9}
	10	670 1073	41.50	1.03×10^{0}	0.87	1.78×10^{-8}
	15	670 1073	38.64	1.11×10^{0}	0.92	1.49×10^{-8}
Olive pits	5	670 1073	46.40	1.01×10^{0}	0.98	6.44×10^{-9}
	10	670 1073	24.10	1.01×10^{0}	0.89	1.49×10^{-8}
	15	488 578	49.34	3.50×10^{0}	0.98	6.01×10^{-9}

Table 3. Pre-exponential factor and activation energy obtained and the statistical parameter values for char gasification stage.

varied from 0.15 to 0.3, SBR from 0 (gasification with air only) to 3, and gasifier temperature in the range of 650–950°C. The moisture content of wastes was set at about 6% by weight.

5.1. Influence of gasifier temperature

In order to analyze the syngas composition and exergetic efficiency with the gasifier temperature variation, SBR value was set at 2, and the ER value was 0.25. **Figure 10** shows that the

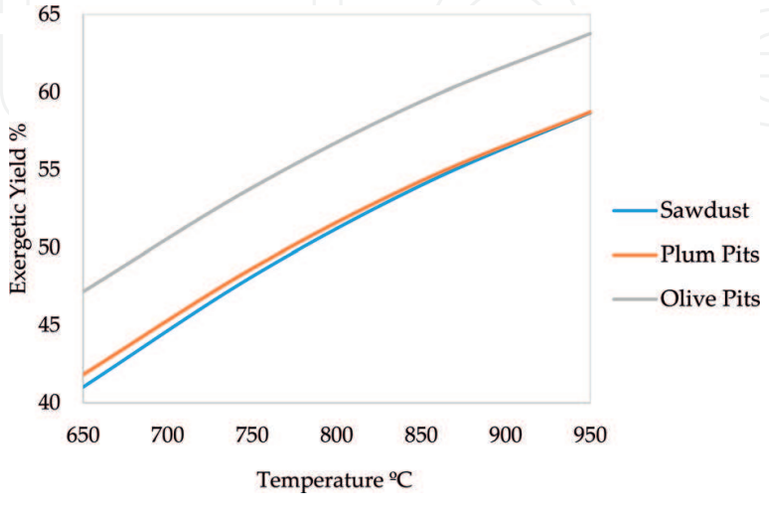

Figure 10. Exergetic yield vs. temperature.

exergetic efficiency increases when the gasifier temperature augments. This is consistent with Zhang results [33]; he informed that higher efficiencies can be achieved by increasing the gasification temperature. In the studied temperature range, the highest value to this parameter was calculated for olive pits (64% at a temperature equal to 950°C), and the lowest value was predicted for the sawdust (41% at a temperature equal to 650°C). The lower temperatures favor the exothermic reactions of CH_4 and CO_2 formations. The higher temperatures favor the endothermic reactions as the H_2 and CO formation reactions. Therefore, in the product, moles of H_2 and CO increase and consequently the exergy efficiency of the process. Therefore, the molar fraction of these gases in the syngas increases the process' exergy efficiency.

5.2. Influence of ER

To study the *ER* influence on the gasification efficiency and syngas composition, the gasifier temperature was set at 850°C and *SBR* at 1.5. **Figure 11** shows that the exergetic efficiency diminishes with the increase of *ER*. It is because the O_2 content in the gasifying agent promotes the combustion reactions. During the gasification process, these reactions are not desirable because they compete with the reactions to transform the biomass in syngas rich in H_2 and CO contents. Increasing the *ER* value, H_2, CO, and CH_4 contents decrease; thus the calorific value of the produced gas and the exergetic efficiency decrease. In addition, the CO_2 and H_2O presences in the syngas composition diminish its calorific value and the exergetic efficiency. For the Olive pits, when *ER* increases, the H_2 and CO contents in syngas decrease about 20% and 15%, respectively.

5.3. Influence of SBR

Considering the influence of *SBR* in the gasification efficiency and syngas composition, this parameter was varied when *ER* value was equal to 0.25 and the gasifier temperature equal to 850°C. **Figure 12** shows the exergetic efficiency decrease with the growth of *SBR*. The lowest value of this parameter corresponds to *SBR* = 1.5; then the exergetic efficiency value increases

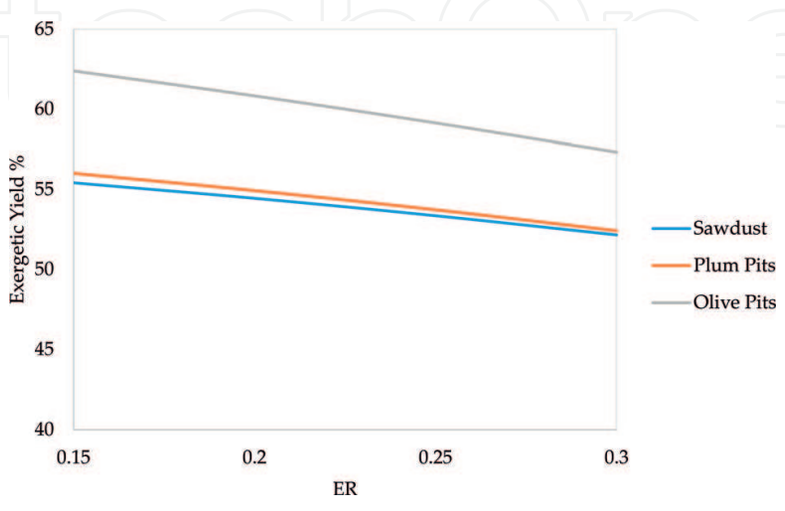

Figure 11. Exergetic yield vs. equivalent ratio (ER).

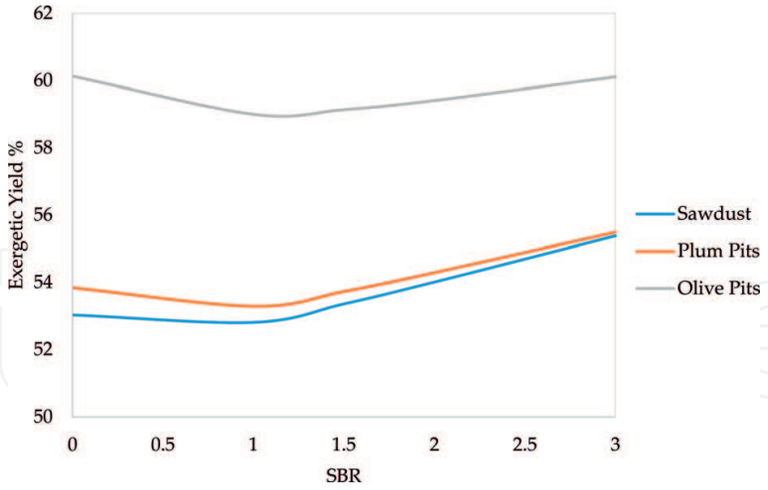

Figure 12. Exergetic yield vs. steam/biomass ratio (SBR).

softly. The decrease is due to the physical exergy of the steam used as the gasifying agent. This decrease is produced because it is necessary to supply energy to the water to transform it in steam. Then, it is partially offset by the increase of H_2 content in the produced syngas.

Comparing the gasification process of olive pits (*SBR = 0*) using air as gasifying agent and an steam–air mixture (*SBR = 1*), the CO content into the produced syngas decreases 38% approximately when the mixture is used; however, the H_2 content increases around 31%.

For the Olive pits, exergetic efficiencies equal to 60.13% and 60.11% were obtained for air and steam/air (SBR = 3) gasification, respectively, considering that the variation is not very noticeable. Physical exergy is related to the syngas sensible heat, and this is lost when the gas cools and it influences the exergetic efficiency value. Increasing the SBR value, the water content in the produced gas flow increases, and also it contributes to the physical exergy. The exergy content of syngas is the sum of physical and chemistry exergies. The physical exergy of biomass steam gasification is higher than the exergy of air gasification due to the higher temperature of the steam, resulting in the exergetic efficiency of air gasification higher to the efficiency of steam gasification.

6. Conclusions

- Two main stages defined the thermal process, named pyrolysis and gasification.
- When heating rate increases, the TG curves are shifted to the right, to the higher temperature region, and the peak height of the DTG curves increases. This shifting occurs because sample solid requires more reacting time at high heating rates.
- To describe the kinetic behavior during the pyrolysis stage, different models were selected. The three-dimensional diffusion (Ginstling-Brounstein) model showed the best fitting for all experiments, assuming that the diffusion is the controlling step of the reaction rate. The kinetic parameters were calculated using this model.

- The variation of E values with the heating rate indicates the existence of a complex multistep mechanism that occurs in the solid state.
- The results of the proposed model suggest to work at high temperatures using an air-vapor mixture as gasifying agent. While the vapor increases the H_2 content in the produced syngas, the exergetic efficiency decreases due to the necessary energy to convert water into steam.

Author details

Rosa Ana Rodriguez*, Germán Mazza, Marcelo Echegaray, Anabel Fernandez and Daniela Zalazar García

*Address all correspondence to: rrodri@unsj.edu.ar

Instituto de Ingeniería Química, Facultad de Ingeniería, Universidad Nacional de San Juan, San Juan, Argentina

References

[1] Berndes G, Hoogwijk M, van den Broek R. The contribution of biomass in the future global energy supply: A review of 17 studies. Biomass and Bioenergy. 2003;**25**:1-28

[2] Ma L, Wang T, Liu Q, et al. A review of thermal–chemical conversion of lignocellulosic biomass in China. Biotechnology Advances. 2012;**30**:859-873

[3] McKendry P. Energy production from biomass (part 1): Overview of biomass. Bioresource Technology. 2002;**83**:37-46

[4] Ellis N, Masnadi MS, Roberts DG, et al. Mineral matter interactions during co-pyrolysis of coal and biomass and their impact on intrinsic char co-gasification reactivity. Chemical Engineering Journal. 2015;**279**:402-408

[5] Han J, Kim HJ. Pyrolysis characteristic and kinetic of sawdust-polypropylene blend. Energy Sources, Part A: Recovery, Utilization, and Environmental Effects. 2009;**31**: 364-371

[6] Edreis EMA, Yao H. Kinetic thermal behaviour and evaluation of physical structure of sugar cane bagasse char during non-isothermal steam gasification. Journal of Materials Research and Technology. 2016;**5**:317-326

[7] Echegaray ME, Castro CM, Mazza GD, et al. Exergy analysis of syngas production via biomass thermal gasification. International Journal of Thermodynamics. 2016;**19**: 178-184

[8] AW C, JP R. Kinetic parameters from thermogravimetric data. Nature. 1964;**201**:68-69

[9] Fernandez A, Saffe A, Pereyra R, et al. Kinetic study of regional agro-industrial wastes pyrolysis using non-isothermal TGA analysis. Applied Thermal Engineering. 2016;**106**: 1157-1164

[10] Marquardt DW. An algorithm for least-squares estimation of nonlinear parameters. Journal of the Society for Industrial and Applied Mathematics. 1963;**11**:431-441

[11] Levenvrg K. A method for the solution of certain non-linear problems in least squares. Quarterly of Applied Mathematics. 1944;**2**:164-168

[12] Zainal ZA, Ali R, Lean CH, et al. Prediction of performance of a downdraft gasifier using equilibrium modeling for different biomass materials. Energy Conversion and Management. 2001;**42**:1499-1515

[13] Ried P, Prausnitz. The Properties of Liquids and Gases. 5th ed. New York: The McGraw-Hill; 2001

[14] Il LY, Do LU. Quasi-equilibrium thermodynamic model with empirical equations for air-steam biomass gasification in fluidized-beds. Fuel Processing Technology. 2014;**128**:199-210

[15] Abuadala A, Dincer I, Naterer GF. Exergy analysis of hydrogen production from biomass gasification. International Journal of Hydrogen Energy. 2010;**35**:4981-4990

[16] Allesina G, Pedrazzi S, La Cava E, et al. Energy-based assessment of optimal operating parameters for coupled biochar and syngas production in stratified downdraft gasifiers. In: The 15th International Heat Transfer Conference Proceedings of the 15th International Heat Transfer Conference. Kyoto, Japan Connecticut: Begellhouse, 2014. Epub ahead of print 2014. DOI: 10.1615/IHTC15.ees.008280

[17] Wu Y, Yang W, Blasiak W. Energy and exergy analysis of high temperature agent gasification of biomass. Energies. 2014;**7**:2107-2122

[18] Prins MJ, Ptasinski KJ, Janssen FJJG. Thermodynamics of gas-char reactions: First and second law analysis. Chemical Engineering Science. 2003;**58**:1003-1011

[19] Moran S. Fundamentals of Engineering Thermodynamics. 5th ed. The Atrium, Southern Gate, Chichester: Wiley; 2006

[20] Hyman D. Heat capacity and content of tars and pitchs. Industrial and Engineering Chemistry. 1959:1764-1768

[21] Eisermann W, Johnson P, Conger WL. Estimating thermodynamic properties of coal, char, tar and ash. Fuel Processing Technology. 1980;**3**:39-53

[22] de Souza-Santos ML. Solid Fuels Combustion and Gasification–Modeling Simulation and Equipment Operation. Boca Raton: CRC Press; 2004 Epub ahead of print 2004. DOI: 176548

[23] Cengel Y, Boles M. Loose Leaf for Thermodynamics: An Engineering Approach. 8th ed. New York: McGraw-Hill Education; 2014

[24] Ptasinski KJ, Prins MJ, Pierik A. Exergetic evaluation of biomass gasification. Energy. 2007;**32**:568-574

[25] Stepanov VS. Chemical energies and exergies of fuels. Energy. 1995;**20**:235-242

[26] Sheng C, Azevedo JLT. Estimating the higher heating value of biomass fuels from basic analysis data. Biomass and Bioenergy. 2005;**28**:499-507

[27] Mason DM, Gandhi KN. Formulas for calculating the calorific value of coal and coal chars: Development, tests, and uses. Fuel Processing Technology. 1983;**7**:11-22

[28] Richard N, Thunman H. General equations for biomass properties. [Internet]. 2002. Available from: http://www.unece.lsu.edu/biofuels/documents/2003-2006/bf03_011.pdf

[29] Amutio M, Lopez G, Aguado R, et al. Kinetic study of lignocellulosic biomass oxidative pyrolysis. Fuel. 2012;**95**:305-311

[30] Jayaraman K, Gökalp I. Pyrolysis, combustion and gasification characteristics of miscanthus and sewage sludge. Energy Conversion and Management. 2015;**89**:83-91

[31] Sanchez-Silva L, López-González D, Garcia-Minguillan AM, et al. Pyrolysis, combustion and gasification characteristics of Nannochloropsis gaditana microalgae. Bioresource Technology. 2013;**130**:321-331

[32] Baker EG, Mudge LK. Mechanisms of catalytic biomass gasification. Journal of Analytical and Applied Pyrolysis. 1984;**6**:285-297

[33] Yaning Z, Bingxi L, Hongtao L, et al. Exergy analysis of biomass gasification with steam/air: A comparison study. 2010 International Conference on Digital Manufacturing & Automation 2010;**1**:678-681

IntechOpen